Thread based electrofluidic platform for direct metabolite analysis in complex samples

*Joan M. Cabot, Michael C. Breadmore, and Brett Paull**

ARC Centre of Excellence for Electromaterials Sciences (ACES) and Australian Centre for Research on Separation Science (ACROSS), School of Physical Sciences, Faculty of Science, Engineering and Technology, University of Tasmania, 75 Private Bag, Hobart, TAS 7005, Australia.

Corresponding author:

Prof. Brett Paull

School of Physical Sciences, University of Tasmania, 75 Private Bag, Hobart 7001, Australia

Ph +61 3 6226 6680; Fax +61 3 6226 2858

E-mail: brett.paull@utas.edu.au

HIGHLIGHTS

- Electrophoretic separations were investigated and employed upon 8 commercial threads.
- Direct, rapid and inexpensive assay for separation and determination of metabolites.
- Separation and quantification of riboflavin from urine was achieved in less than 2 minutes.
- Thread-based devices exhibited a linear working range 0.1-5 μg/mL and good correlation with standard method.

ABSTRACT

The application of electrophoresis upon commercial threads is investigated for development of low-cost diagnostics assays, designed for the matrix separation and quantification of low abundance metabolites in complex samples – in this work riboflavin in human urine. Zone electrophoresis was evaluated upon 8 commercially available threads, with several synthetic threads exhibiting higher electroosmotic flow (EOF) and increased electrophoretic mobility of the rhodamine 6G, rhodamine B, and fluorescein. Of those tested, a nylon bundle was selected as the best platform, offering less band dispersion and higher resolution, a high relative EOF, whilst minimising the contribution of joule heating. A novel 3D printed platform was designed, based on a modular system, facilitating the electrophoresis process and rapid assembly, whilst offering the potential for multiplexed analysis or investigation of more complex systems. Using the thread-based electrophoresis system, riboflavin was determined

in less than 2 minutes. The device exhibited a linear working range from 0.1 to 15 μg/mL of riboflavin in urine, and was in good agreement with capillary electrophoresis measurements.

KEYWORDS

Microfluidic thread based analytical device; thread electrophoresis; riboflavin; urine analysis; metabolite analysis; 3D printed platform.

1. INTRODUCTION

Recent advances in functional materials, and their application in the field of diagnostics and sensors, is driving the development of smart 'wearables' and interactive textiles. This exciting area of research has many possible applications, with the integration of sensors in clothing offering the potential to provide real-time data on the interaction and exposure of the wearer to his/her environment, plus significant opportunities for personal health monitoring. Consequently, there is extensive interest in the development of minimally invasive, accurate, durable, user-friendly, and low cost thread and textile based diagnostic platforms [1–3].

Thread and textiles have gained considerable attention as potential low cost substrates for microfluidics and biosensor applications. Hydrophilic threads do not require external forces to transport aqueous fluids and most threads are flexible and thus can be easily incorporated or woven into various textile supports. Additionally, threads can be readily disposed of after use, are readily mass produced, and easily functionalised, coated or extruded in varying formats, from a wide variety of starting materials, both natural and synthetic [2–13]. Due to this simplicity and functionality, a variety of applications have been demonstrated using two main platforms over the last few years. First, and similar to paper-based microfluidics, are the two dimensional patterned or woven fabric-based microfluidic devices [14–23]. The second group are based upon single threads, which generally involve much smaller solution volumes, as in these examples the flow within the strands of the thread is confined to one direction. The use of this later platform has been applied to bacteria isolation and quantification [24], chemotaxis studies for cell culture systems [25], immunoassays [26,27], blood typing [28], chemical

64 synthesis [29], and the determination of nucleic acids [30,31], proteins [4,7,29,31–34], glucose
65 [29,35–37], drugs [38], small ions [6,8,32,39] and metals [40]. Several detection techniques
66 have been used for these various applications, with the most common, albeit the least sensitive,
67 being simple colorimetric detection. To achieve gains in sensitivity more complex approaches
68 have also been demonstrated, involving the use of immobilised gold nanoparticles [31,41],
69 electroanalytical detection [42], electrochemiluminescense [21], and fluorescence [24].
70 However, in most applications involving complex samples, e.g. biological samples, such as
71 blood, sweat or urine, the separation of the target solute(s) from interferences within the
72 matrix is required [43–47].

73 In this paper, the controlled transport of fluids and target solutes using thread-based
74 electrophoresis was investigated across a diverse set of commercially available threads, from
75 different materials to different structures. The study aimed to identify the optimum material,
76 sample loading procedure, and conditions for thread electrophoresis, and apply the technique
77 in a biological assay. In this regard, the technique was applied to the separation, detection and
78 quantification of vitamin B2 within urine. Vitamin B2 or riboflavin is on the World Health
79 Organization's (WHO) List of Essential Medicines [48], since it plays major roles in energy
80 production; cellular function, growth, and development; metabolism of fats, drugs, and
81 steroids; and help to maintain normal levels of homocysteine and amino acid in the blood.

82

83 ## 2. EXPERIMENTAL SECTION

84 ### *2.1. Materials and Reagents*

85 Tris-(hydroxylmethyl)amino-methane (TRIS), 2-(cyclohexylamino)-ethanesulfonic acid
86 (CHES), sodium hydroxide, riboflavin, rhodamine 6G, rhodamine B, fluorescein sodium salt,
87 and acetonitrile, each of analytical reagent grade, were obtained from Sigma-Aldrich (New
88 South Wales, Australia). Disodium tetraborate decahydrate was purchased from Merck
89 Millipore (Darmstadt, Germany). Solutions were prepared in water from a Milli-Q Water Plus
90 system from Millipore (Bedford, MA, USA), with a resistivity of 18.2 MΩ cm.

91 100 % nylon bundle (diameter (Ø) 803 ± 53 µm, woolly nylon stretch overlocking thread,
92 QA thread, China), 100 % silk (Ø 573 ± 38 µm, stranded silk, 8.4 yd, Cascade House, Australia),
93 100 % cotton (Ø 397 ± 19 µm, mercerised twice, 8.7 yd, mouliné stranded, DMC, France),
94 100% polyester (Ø 282 ± 12 µm, 110 yds/vgs, Gütermann GmbH, Germany), 100% acrylic (Ø
95 671 ± 58 µm, 4 ply, Marvel Soft Baby, Bella Baby, Turkey), 50% acrylic 50% nylon (Ø 618 ±
96 39 µm, 4 ply, Bambini, Bella Baby, Turkey), 100% pure Merino wool (Ø 581 ± 55 µm, 45 yards
97 per skein, Bella Lusso, Italy), waxed dental tape (1455 ± 29 µm wide and 150 µm thick, VITIS®,
98 Dentaid, Spain), were each evaluated for thread-based microfluidics. Diameters of the wetted
99 threads were measured across 10 different samples using an objective-type inverted
100 microscope (Nikon Eclipse TE2000). In order to clean and eliminate impurities, threads were
101 prewashed in Milli-Q water and sonicated for 10 minutes, in triplicate, and again rinsed with
102 Milli-Q water. In order to study the properties of the raw material, threads were not
103 chemically or plasma treated.

104 Two separate urine samples were prepared, a blank (fresh non-spiked urine sample from a
105 healthy donor) and spiked sample (blank urine spiked with 8 µg mL^{-1} riboflavin). Stock

106 solutions of riboflavin were prepared in water and the standards for calibration in the
107 appropriate buffer solution, over the range 0.1 to 15 μg mL^{-1} (or ppm). All stock, standards and
108 sample solutions were stored in dark and refrigerated at 4 °C.
109
110 ***2.2. Platform design***
111 The platform design developed herein provides a versatile modular system for thread-based
112 microfluidics (Figure 1). The discrete buffer reservoirs provide for an interconnected and
113 robust thread arrangement which facilitating rapid assembly, whilst offering the potential to
114 construct complex thread-based microfluidic systems. The base was 12 cm × 8 cm × 1 cm
115 (width × depth ×height) and was accurately designed to fit both a microscope slide support and
116 a Dino-Lite handheld digital microscope. The platform itself contained 90 pin-holes and an
117 empty detection zone in the middle. The movable buffer reservoirs have a hoop to tie in the
118 thread, a cylinder to introduce the electrode, horizontal rollers to guide the thread to the lower
119 part of the reservoir, and a basin allowing a maximum of 750 μL of buffer, keeping the thread
120 hydrated during the analytical process. The thread was then placed in suspension, parallel to
121 the base, and approximately 1-2 mm higher than the buffer level, avoiding wicking between
122 the reservoirs and thread from over-hydration. Additionally, electroosmic flow facilitated the
123 flux of fresh buffer solution minimising solvent evaporation. Cylindrical pins were placed
124 underneath to fix the reservoir on the base. Figure 1 shows the CAD designs and photographs
125 for the reservoir, platform, and final set up, with two reservoirs and a single thread under the
126 fluorescent microscope. Base and buffer reservoirs were designed using SolidWorks CAD

127 software (SolidWorks Corp., Dassault Systemes, France). Designs were 3D printed using an
128 Eden 260VS (Stratasys, MN, USA) with VeroClear build material, and SUP707 water soluble
129 support. Support material was removed by agitation in 2 % NaOH for 2 hours, followed by 4-
130 6 hours in water. Finally, printed parts were rinsed and subsequently soaked for 1 day in Milli-
131 Q water.
132

133 ***2.3. Choice of thread***

134 Electrophoresis can be carried out upon a wide range of commercial threads, each providing
135 unique physical and chemical properties, which translate to differing electrophoretic
136 behaviour and selectivity. The electrophoretic properties of eight types of thread were
137 examined: nylon bundle (NYL), silk (SE), cotton (CO), wool (WO), acrylic (AC), 50%
138 acrylic/50% nylon (AC/NYL), polyester (PES), and waxed dental tape (WT). Threads
139 investigated were selected based upon their ability to create a liquid pathway, their strength,
140 flexibility, absorbency, commercial availability, low-cost, malleability, and durability.
141 Similarly, variation was sought between filament structure and arrangement to form the
142 thread. Figure 2 shows scanning electronic micrograph (SEM) images of the different threaded
143 materials used in this study.
144

145 ***2.4. Thread electrophoresis system operation***

146 All experiments were carried out at constant voltage and in cathodic mode, where the anode
147 was in the inlet and the cathode was in the outlet buffer reservoir. Voltage was applied using

148 an in-house built 4-channel (0-5kV) DC power supply. The system was interfaced to the
149 computer using a 12-Bit, 10 kS/s multifunction DAQ system (USB-6008 OEM, National
150 Instruments, Austin, TX, USA) and data acquisition was achieved using software LabView
151 v11.0. Temperature increases due to Joule heating effects were monitored with a FLIR E40
152 MSX infrared camera (Notting Hill, VIC, Australia). A USB microscope AM4113T-GFBW
153 (Dino-Lite Premier, Clarkson, WA, Australia) fitted with a blue light-emitting diode for
154 excitation and a 510 nm emission filter was used to take fluorescence images and videos. The
155 microscope objective was fixed at 30X and the thread image focused by adjusting the distance.
156 ImageJ (National Institutes of Health, http://rsb.info.nih.gov/ij/) was used to analyse the region
157 of interest (ROI) and then monitor the mean fluorescence intensity value of the ROI versus
158 time. Note that since background is black, its signal intensity is valued 0.

159 To prepare the thread for separations, three simple steps were followed. The first, was to set
160 and tighten the thread with respect to the reservoir. Reservoirs were located and attached to
161 the base according to the desired thread length. One end of the thread was knotted with the
162 ring of the first reservoir, passed below its rollers and directed to the second reservoir.
163 Afterwards, the thread was guided below the rollers of the second reservoir and knotted
164 around its ring (Figure 1). The second step involved pre-rinsing the thread with the
165 appropriate buffer. Since the reservoirs are detachable, both reservoirs and attached thread
166 were submerged into a vial full of buffer and shaken for 1 minute. Since threads were entirely
167 soaked in buffer, they were completely wetted regardless of the relatively low hydrophilicity
168 indexes of some of the threads. The third step was to gently shake the reservoirs and thread to

169 remove any excess of buffer, and relocate them in the platform. Finally, 500 μL of working
170 buffer solution was added into each of the reservoir chambers. Before applying voltage, the
171 system was left for 1 minute in order to achieve equilibration and to avoid any capillary based
172 flow across the thread during its subsequent application. For electrophoretic separations, two
173 electrodes were introduced through the reservoir cylinder and connected to the system.
174 Voltage was then applied and current measurements monitored using LabView. When the
175 separation was complete, both the reservoirs and thread could be simply detached from the
176 base, submerged into a water vial for 2 minutes, followed by 2 minutes in fresh buffer and then
177 applied to a new separation. At the end of the day, reservoirs and thread were cleaned with
178 water, air-dried, and stored for further usage.
179
180 ***2.5. Electroosmotic and electrophoretic mobility measurement***
181 There are several methods to measure the electroosmotic flow (EOF) in microfluidic systems
182 [49,50]. Herein, the Kohlrausch regulating function (KRF) [51] was used, based on the
183 measurement of changes in current signal from the introduction of a buffer-like solution. The
184 thread was wetted with a solution of 2.5 mM of Tris/CHES buffer, whereas the reservoir at the
185 injection end of the thread contained a buffer with slightly higher ionic strength, 2.6 mM.
186 When an external electric field (E = 200 V/cm) was applied, the solution in the injection
187 reservoir flowed into the thread and the electric current in the circuit changed when the total
188 conductivity in the thread changed. When inlet solution covered the entire thread, the electric

189 current was constant. EOF mobility (μ_{EOF}) was calculated according to the time (t_0) that the

190 buffer was displaced by the one in the injection reservoir and the thread length (L_T):

191 $$\mu_{EOF} = \frac{L_T}{t_0 E} \quad (1)$$

192 For accurate current measurements, a very small resistor (10.0 kΩ) was inserted between the

193 reservoir electrode and ground. Measured voltage across the resistor was converted to current.

194 5% differences between buffer concentrations was sufficient to detect the current variation.

195 Charged solutes experience an electrophoretic mobility (μ_{ep}), based on the charge/size ratio

196 of the ions. Therefore, the apparent mobility (μ_{ap}) is obtained from the sum of both μ_{EOF} and

197 μ_{ep}. To determine the μ_{ap}, 0.5 µL of sample was dropped at 1 cm along a 6 cm long thread.

198 Samples of 10 µM rhodamine 6G (Rh6G), 10 µM rhodamine B (RhB), and 3 µM fluorescein

199 (FL) were prepared separately using a 2.5 mM Tris/CHES buffer solution. When the electric

200 field was applied, the sample was driven to the cathode and light intensity measured using a

201 USB Dino-Lite microscope at 5 cm from inlet reservoir. Migration time (t_m) was measured

202 using the maximum peak intensity of the electropherogram. μ_{ap} was calculated as follows:

203 $$\mu_{ap} = \frac{L_D}{t_m E} = \mu_{EOF} + \mu_{ep} \quad (2)$$

204 where L_D is the effective length that sample has travelled.

205

206 ***2.6. Urine assay in thread electrophoresis***

207 To determine riboflavin in urine, 0.5 µL of untreated urine was directly applied onto the

208 thread at 1.0 ± 0.1 cm from the inlet reservoir, with a thread of 6 cm total length and using 5

209 mM Tris/CHES as the separation buffer (pH 8.8, ionic strength 0.80 mM, conductivity 4.16 10^{-}

210 ^{3} S/m). No current variations and solvent evaporation were observed after 20 minutes of
211 operation. The sample, without any pretreatment, was directly dropped from an automated
212 eVol XR digital analytical micro-syringe (Trajan Scientific and Medical, Melbourne, Australia)
213 onto the thread surface, using a 5 µL total volume syringe (0.2-5 µL dispense volumes).
214 Accuracy and reproducibility of the syringe is reported as ± 1% (SGE Analytical Science,
215 Australia). A detection point was fixed at 4.5 ± 0.1 cm from the inlet reservoir. A fluorescence
216 microscope (Eclipse Ti-U, Nikon, Tokyo, Japan) with an objective 20X was used to focus on
217 the thread. An electric field of 300 V/cm was applied. Quantitative measurements were
218 achieved using a photomultiplier tube (Hamamatsu Photonics KK, Hamamatsu, Japan)
219 connected to the microscope. Data acquisition was made using an Agilent interface (35900E)
220 connected to a laptop and operated by Agilent ChemStation software (Agilent Technologies,
221 Waldbronn, Germany). The excitation wavelength was 482 nm and emission detected at 523
222 nm (Semrock, Rochester, NY, USA). In order to determine the concentration of riboflavin, a
223 series of standard solutions were prepared from 0.1 to 15 µg/mL in buffer solution. After 5
224 runs, reservoirs and thread were detached from the base and rinsed as mentioned above.
225

226 ***2.7. Urine assay in capillary electrophoresis***

227 Capillary electrophoresis (CE) separations were carried out on a Beckman Coulter (Fullerton,
228 CA, USA) P/ACE MPQ CE System equipped with a laser induced fluorescence detector (LIF)
229 at 488 nm. The analytical procedure was modified from previous work [52]. Briefly,
230 experiments were conducted using a bare-fused silica capillary (Polymicro Technologies, AZ,

231 USA) of 100 µm I.D. (360 µm O.D.) with a total length of 65.2 cm (effective length to detector,
232 55 cm). The capillary was maintained at a constant temperature of 25.0 ± 0.1 ºC. Sample and
233 standards were injected using hydrodynamic pressure of 0.5 psi for 3s. Separation was carried
234 out at 18kV and normal polarity. Prior to analysis, the capillary was preconditioned as
235 following: 1 M NaOH (10 min), Milli-Q water (5 min), and buffer (10 min). Between
236 consecutive injections the capillary was conditioned with buffer (3 min). At the end of each
237 run, the capillary was post-conditioned with 0.1M NaOH (5 min) and H_2O (10 min). The
238 separation buffer was prepared from a solution of water/acetonitrile (9:1 v/v) containing 10
239 mM borate (pH 9.6 adjusted with 0.1 M NaOH).

240 In order to avoid capillary blockage and sample matrix related issues, urine samples (10 mL)
241 were pre-treated by centrifuging at 8000 rpm for 15 minutes (model Eppendorf 5424,
242 Hamburg, Germany), and the supernatant filtered using 0.45 µm size porous filters (Millex-
243 HA, Merc Millipore, Darmstadt, Germany). The filtered extract was collected and stored in a
244 refrigerator prior to analysis.

245

246 3. RESULTS AND DISCUSSION

247 ***3.1. Buffer, current and thread considerations***

248 Electrophoretic processes within and upon threads strongly depend on several factors:
249 surface polarity, chemical composition, microstructure of the thread, porosity and amount of
250 specific surface area, and swelling properties in water. Hence, the material used and the applied
251 conditions will determine the electroosmotic flow and apparent mobility along the thread. To

252 achieve electrophoresis upon the thread there must be: 1) a homogenous buffer pathway
253 between electrodes; and 2) the electrical resistivity of the thread must be higher than that of
254 the buffer. Accomplishing these two requirements, it is also important to consider that when
255 voltage and ionic concentration is high, joule heating can be significant, providing a
256 disproportionate increase in current with voltage, and a non-linear Ohm's law dependency.
257 This Joule heating can cause solvent evaporation, band broadening and potential thread
258 degradation. To reduce the Joule effect it is important to select the appropriate buffer. In this
259 work, Tris and CHES buffers were selected, since both have strong buffering capacity over the
260 pH range 8-9, but low conductivity and low ion mobility, which limits the extent of joule
261 heating. Current and temperature were measured at electric fields between 0-500 V/cm, at
262 concentrations of 1-20 mM of Tris/CHES buffer. Conductivity values ranged from 9.38 10^{-4} to
263 1.60 10^{-2} S/m, ionic strength from 0.16 to 3.26 mM, and buffer capacity from 0.62 to 12.58 mM.
264 Buffers with higher concentrations, > 5 mM, generated higher Joule heating, as evident from
265 the observed Ohm's law dependences and temperatures measurements taken using the IR
266 camera (see Figure S-1 in ESI†).

267 Joule heating can also be minimised by reducing the diameter of the thread. However,
268 extremely small diameters are not practical, principally due to the reduced sample loading
269 capacity and detection window. The Ohm's Law dependences for 8 different threads, with
270 diameters ranging between 250 and 800 μm, were examined for electric fields up to 500 V/cm
271 (Figure 3a). Linearity was achieved in all cases bar acrylic, which clearly showed a deviation
272 for E over 400 V/cm. In order to identify resistivity differences between thread types, current

273 values were also plotted as a function of the cross sectional area of the threads (Figure 3b).
274 Here, with the exception of the response seen for the NYL, the overall linearity demonstrates
275 that the current is principally dependent upon the thread diameter rather than the chemical
276 composition of the material. Nevertheless, small differences can be observed, for instance WT
277 and AC/NYL show a reduced dependence and acrylic slightly higher relative relationship. On
278 one hand, these deviations can potentially reflect variations in wettability due to the differing
279 surface chemistry of the materials. As in the case of AC, R-CN functional groups are very polar,
280 increasing electrolyte penetration. By adding a 50% nylon into the structure, R-CONH-R'
281 amide groups decrease its polarity slightly and so wettability is reduced. On the other hand,
282 thread density also needs to be considered. Looser arrangements, such as the AC filaments
283 (Figure 2-v) can retain larger volumes of electrolyte. In contrast, the planar WT structure, 150
284 μm thick (Figure 2-viii), is a considerably tighter thread and therefore holds a lower volume
285 of electrolyte and therefore less current. Regarding the nylon bundle, big deviations were
286 observed, with a current decrease of approximately 53% from the linear trend. Calculating the
287 theoretic diameter from the experimental current values using the regression parameters from
288 Figure 3b, suggests the nylon bundle contains ~ 24% less liquid than the other materials.
289

290 ***3.2. Electroosmotic flow and ion mobility***

291 Shown in Figure 3c are the μ_{EOF} and μ_{ap} profiles for three different solutes (Rh6G: positive,
292 RhB: zwitterionic and FL: negative) observed upon the different threads investigated. These
293 data and standard deviations are also summarised in Table 1. Values obtained reveals that the

294 μ_{EOF} for all threads exhibited a significant cathodic EOF to transport all solutes, cations, neutral
295 components and anions ($\mu_{EOF} > |\mu_{ep(anion)}|$), across the detector region. The highest EOF values
296 were recorded for NYL and WT followed by the acrylic-based thread, PES, and finally the
297 natural threads (SE, CO and WO). Due to their controlled manufacturing processes, synthetic
298 threads have regular structures (Figure 2b) and presumably a more homogeneous surface
299 chemistry. On the contrary, natural threads have irregular filaments shapes, and many intra-
300 fibrillar gaps, providing irregular microfluidic channels. CO has a hollow ribbon like
301 appearance with cellulose filaments, and wool is composed of protein with crimps in the
302 outside surface of the filament like a series of serrated scales (Figure 2-iii, iv). As an exception,
303 SE revealed a higher μ_{EOF}, and it possesses a triangular prism-like filament with regular
304 microfluidic channels (Figure 2-ii). Regarding solute μ_{ap}, with both CO and WO, solute-surface
305 interactions were evident, which may be related to both surface chemistry and the more
306 irregular and porous thread structure. Positively charged solutes in silk presented similar
307 behaviour, whilst FL reached a mobility of 1.9 ± 0.1 (10^{-8} m^2 V^{-1} s^{-1}). Silk is mainly composed
308 of fibroin protein. The low isoelectric point of silk (3.5) and high concentration of glycine (not
309 sterically constrained) allows tight packing, creating high levels of interaction with positive
310 solutes and EOF as high as that seen with polyester.

311 Comparing EOF recorded with each of the synthetic threads, higher values are expected for
312 those with higher electronegativity or zeta potential, lower swelling properties [53] and
313 smooth microstructure that ease the liquid flow. Therefore, the PES material with the lowest
314 ionisation capacity and charge density, due to ester groups (-R-COO-R'-), showed the lowest

315 μ_{EOF}. Similarly, since NYL (R-CONH-R'-) has lower electronegativity than AC (-R-CN), higher
316 values were observed for the acrylic thread than the AC/NYL threads, even though AC showed
317 clearly higher swelling properties. However, the NYL and WT presented the highest values,
318 and a reasonable explanation for this behaviour must lie with structural differences (Figure
319 2a). It is possible that the greater alignment of the filaments in tape, or the greater physical
320 spaces within the bundle, facilitated bulk solution flow with less physical impediments, and
321 thus delivered higher mobility values. Regarding μ_{ap}, strong surface interactions were not seen
322 with any of the synthetic threads, although some retardation was observed for RhB with
323 polyester, which had a lower value than negative compounds such as FL. For acrylic, RhG6
324 and RhB mobilties were slightly lower than expected, whereas AC/NYL showed higher
325 resolution between the three solutes. Significant apparent mobility differences were also
326 observed between the NYL and WT.

327 Overall, synthetic threads (NYL, AC, WT, AC/NYL and PES) showed higher μ_{EOF} than
328 natural ones (SE, CO, and WO), with the acrylic-based thread exhibiting the highest.
329 However, filament aggregation is also important as bundles and tapes offered less obstructions
330 and provided increased EOF. Additionally, higher resolution and $|\mu_{ep}|$ was shown for nylon-
331 based thread than others, such as acrylic and polyester. Consequently, the examination of
332 several types of threads established that the nylon bundle was a suitable material for
333 electrophoresis and solute separations. Other reasons such as low current, durability, and easy
334 handling, make nylon bundle the preferred option.

335

336 ***3.3. Sample loading***

337 Several loading strategies were studied in order to achieve the best loading efficiency
338 (smallest sample band width upon the thread). Similar to cross-channels used in microchip
339 electrophoresis, sample loading can be carried out by using a secondary loading thread across
340 the main separation thread. Herein, 4 loading strategies were evaluated: 1) a two-step standard
341 loading and separation; 2) a two-step loading and separation with cross-pinching and pull-
342 back, respectively; 3) a two-step standard loading and pull-back separation using lower
343 diameter in the loading channel; 4) the direct application of the sample directly onto a single
344 separation thread. Each of these strategies were optimised separately to the conditions
345 summarised in Figure 4. Table 2 shows all 4 approaches, images taken during the process,
346 electropherograms, full peak width at half maximum (FWHM), and the obtained peak area.

347 The first approach confirmed that capillary action or wicking had a substantial effect.
348 Wicking along the separation channel was significant during sample loading. Under separation
349 conditions, this extended sample band provided both poor peak shape for the solute and a
350 considerable increase in baseline signal. By employing the second approach, pinching and pull-
351 back, the sample wicking effect was greatly reduced, giving a narrower sample band and no
352 changes in baseline. However, in initial experiments the thread diameter used was relatively
353 high, resulting in a high sample volume and therefore relatively high values of FWHM and
354 peak area. In the third approach, a polyester thread with ~ 3 times smaller diameter was used,
355 reducing sample volume up to 65%, and therefore increasing efficiency significantly. The
356 cross-loading approaches provide the capability to perform automated assays of the same

sample without any additional instrumentation, keeping the loading point constant at all times. It is worth noting that loading and separation can be carried out for any of the synthetic threads that have been studied. Movie S-1 in ESI† shows a separation of RhB and FL using the cross-shaped waxed tape.

However, the fourth approach, namely the direct sample application (with automated pipette) provided similar results to approach 3 above, and although a manual approach, had the advantage of both simplicity and avoidance of the secondary thread completely, and the need for an extra voltage supply.

3.4. Analysis of riboflavin in urine

Riboflavin or vitamin B2 is a natural fluorophore which plays crucial roles in certain metabolic reactions, such as in enzymatic processes involving flavin coenzymes. Since it cannot be synthesised within the human body, vitamin B2 depleted diets or poor absorption can result in significant health problems. Extremely low concentration in biological matrices and susceptibility to photodegradation makes riboflavin difficult to quantify. Therefore, separation techniques, such as electrophoresis, as well as selective detection, are essential for the determination of riboflavin in such samples.

As a proof-of-concept, electrophoresis upon the nylon bundle thread with selective fluorescence detection was used for the determination of riboflavin in urine. The thread not only provides the substrate for the separation, but also as a filter/percolation matrix for sample particles and much of the undesired components material within the urine. Sample can be

directly assayed, avoiding any extra steps such as micro-extractions, centrifugation, or sample filtration. By using an automatic micro-pipette, the sample can be accurately loaded, keeping the same loading point and sample volume without the need to stop the voltage or renew the buffer solution within the thread. Movie S-2 in ESI† shows the electromigration of riboflavin along the nylon bundle. A sequence of images can be seen in Figure 5a. Shown in Figure 5b is an electropherogram depicting repetitive sample loading every 45 seconds. As can be seen, baseline and peak shape were constant, with peak area constant after 10 consecutive loadings (493 ± 28, RSD = 5.7%). It was noted however that extended use would result in a gradual change in buffer reservoir levels, and thus it is recommended to rinse and replace buffer solution every 5 loadings to maintain repetitive migration times.

The well-known photochemical reactions involved in the degradation of riboflavin can affect its concentration significantly. Around 30% of the riboflavin in milk is destroyed by sunlight within 30 minutes [54]. To study the separation capabilities of thread electrophoresis, a riboflavin solution of 5 μg/mL was analysed after 1 hour exposure to sunlight. The electropherogram shown in Figure 5c shows the separation of riboflavin from its three common breakdown products - lumiflavin, lumichrome, and carboxymethylflavin, in decreasing order of apparent mobility.

For the diagnostic assay of riboflavin in urine, 0.5 μL of each sample was dropped onto the thread and the signal intensity was monitored using a PMT and Agilent software as per Experimental Section. As a comparison, these samples were also analysed using a standard capillary electrophoresis method on a Beckman CE. Electropherograms obtained by both

399 techniques are shown in Figure 6. Naturally, higher resolution and efficiency were observed
400 from the CE, which uses open capillary channels, an 11 fold longer separation length, 10 times
401 higher voltage, and produces a 20 minute long electropherogram. However, using thread
402 electrophoresis, a quantitative assay was possible, providing a low cost diagnostic capability.
403 Calibration curves from 0.1 to 15 μg/mL for the thread-based and capillary electrophoresis are
404 shown in Figure S-2 in ESI†. As can be seen, the intensity exhibits a linear relationship with
405 concentration, with a correlation > 0.99 (R^2) in both cases. The parameters obtained from the
406 calibration curve were used to determine the riboflavin concentration in urine. Results for the
407 blank were 2.02 ± 0.29 and 2.16 ± 0.08, and spike 9.85 ± 0.88 and 10.13 ± 0.26 for thread
408 electrophoresis and CE, respectively (Figure 7). Values obtained from the simple thread-based
409 platform with direct sample loading were comparable to the ones obtained by the standard CE
410 method. Higher standard deviations were seen for the on-thread repeat assays. The major cause
411 of this was sample introduction. The injection performance of commercial CE instruments
412 remains somewhat superior than that developed to-date with the thread. However, separation
413 and quantification was successfully achieved for vitamin B2 in urine using thread
414 electrophoresis, in under 2 mins, with the simplicity and costs of this thread based platform
415 orders of magnitude lower than the commercial CE instrument, which for a proof-of-concept
416 assay of this nature is deemed highly encouraging.
417

418 4. CONCLUSIONS

419 Electrophoresis was applied on commercial threads for the implementation of low cost,
420 semi-automated determination of low abundant target compounds in biological matrixes.
421 Based on this multifilament substrates, separation was achieved in less than a minute,
422 presenting significant potential for the development of new biosensor and affordable
423 diagnostic devices. Threads were tested using a versatile 3D printed platform, providing rapid
424 simple assembly, while offering great potential for multiplexed analysis. Synthetic threads
425 showed higher EOF, with acrylic (cyanide based) providing the highest value. However, nylon
426 bundle was chosen due to its chemical properties, low solute dispersion and high resolution,
427 whilst also minimising the contribution of Joule heating. As a proof-of-concept study, the
428 approach was applied to the separation and quantification of riboflavin in human urine. Using
429 only 6 cm of thread, with less than 100 μA of current generated, and low sample volume
430 requirements, riboflavin in untreated urine was accurately determined in only 2 minutes.
431

432 ACKNOWLEDGMENTS

433 This work is funded by the Australian Research Council (ARC) Centre of Excellence
434 program and the University of Tasmania (UTas). The authors thank the service from Central
435 Science Laboratory (CSL) for providing SEM equipment and 3D printed facilities. Funding
436 from the Australian Research Council Centre of Excellence Scheme (Project Number CE
437 140100012) is gratefully acknowledged. MCB would like to thank the ARC for a Future
438 Fellowship (FT130100101).

REFERENCES

[1] S. Coyle, Y. Wu, K.-T. Lau, D. De Rossi, G. Wallace, D. Diamond, Smart Nanotextiles: A Review of Materials and Applications, MRS Bull. 32 (2007) 434–442. doi:10.1557/mrs2007.67.

[2] J.R. Windmiller, J. Wang, Wearable Electrochemical Sensors and Biosensors: A Review, Electroanalysis. 25 (2013) 29–46. doi:10.1002/elan.201200349.

[3] A.K. Yetisen, H. Qu, A. Manbachi, H. Butt, M.R. Dokmeci, J.P. Hinestroza, et al., Nanotechnology in Textiles., ACS Nano. 10 (2016) 3042–3068. doi:10.1021/acsnano.5b08176.

[4] T. Narahari, D. Dendukuri, S.K. Murthy, Tunable Electrophoretic Separations Using a Scalable, Fabric-Based Platform, Anal. Chem. 87 (2015) 2480–2487. doi:10.1021/ac5045127.

[5] S. Seyedin, J. Razal, P.C. Innis, A. Jeiranikhameneh, S. Beirne, G.G. Wallace, Knitted Strain Sensor Textiles of Highly Conductive All Polymeric Fibers., ACS Appl. Mater. Interfaces. 7 (2015) 21150–21158. doi:10.1021/acsami.5b04892.

[6] X. Li, J. Tian, W. Shen, Thread as a versatile material for low-cost microfluidic diagnostics, ACS Appl. Mater. Interfaces. 2 (2010) 1–6. doi:10.1021/am9006148.

[7] M. Reches, K.A. Mirica, R. Dasgupta, M.D. Dickey, M.J. Butte, G.M. Whitesides, Thread as a Matrix for Biomedical Assays, ACS Appl. Mater. Interfaces. 2 (2010) 1722–1728. doi:10.1021/am1002266.

[8] M.M. Erenas, I. de Orbe-Payá, L.F. Capitan-Vallvey, Surface modified thread-based microfluidic analytical device for selective potassium analysis, Anal. Chem. 88 (2016) 5331–5337. doi:10.1021/acs.analchem.6b00633.

[9] A. Nilghaz, D.R. Ballerini, W. Shen, Exploration of microfluidic devices based on multi-filament threads and textiles: A review, Biomicrofluidics. 7 (2013) 51501. doi:10.1063/1.4820413.

[10] S. Xing, J. Jiang, T. Pan, Interfacial microfluidic transport on micropatterned superhydrophobic textile., Lab Chip. 13 (2013) 1937–1947. doi:10.1039/c3lc41255e.

[11] D.R. Ballerini, Y.H. Ngo, G. Garnier, B.P. Ladewig, W. Shen, Gold Nanoparticle-Functionalized Thread as a Substrate for SERS Study of Analytes Both Bound and Unbound to Gold, AIChE J. 60 (2014) 1598–1605. doi:10.1002/aic.

[12] L. Guan, A. Nilghaz, B. Su, L. Jiang, W. Cheng, W. Shen, Stretchable-Fiber-Confined Wetting Conductive Liquids as Wearable Human Health Monitors, Adv. Funct. Mater. 26 (2016) 4511–4517. doi:10.1002/adfm.201600443.

[13] A. Nilghaz, L. Zhang, M. Li, D.R. Ballerini, W. Shen, Understanding Thread Properties for Red Blood Cell Antigen Assays : Weak ABO Blood Typing, ACS Appl. Mater. Interfaces. 6 (2014) 22209–22215.

[14] P. Bhandari, T. Narahari, D. Dendukuri, “Fab-chips”: a versatile, fabric-based platform for low-cost, rapid and multiplexed diagnostics., Lab Chip. 11 (2011) 2493–2499. doi:10.1039/c1lc20373h.

[15] S. Lathwal, H.D. Sikes, A Method for Designing Instrument-Free Quantitative Immunoassays., Anal. Chem. 88 (2016) 3194–202. doi:10.1021/acs.analchem.5b04538.

[16] S. Bagherbaigi, E.P. Corcoles, D.H.B. Wicaksono, Cotton fabric as an immobilization matrix for low-cost and quick colorimetric enzyme-linked immunosorbent assay (ELISA), Anal. Methods. 6 (2014) 7175–7180. doi:10.1039/c4ay01071j.

[17] A. Nilghaz, D.H.B. Wicaksono, D. Gustiono, F.A. Abdul Majid, E. Supriyanto, M.R. Abdul Kadir, Flexible microfluidic cloth-based analytical devices using a low-cost wax patterning technique, Lab Chip. 12 (2012) 209–218. doi:10.1039/c1lc20764d.

[18] M. Liu, C. Zhang, F. Liu, Understanding wax screen-printing: A novel patterning process for microfluidic cloth-based analytical devices, Anal. Chim. Acta. 891 (2015) 234–246. doi:10.1016/j.aca.2015.06.034.

[19] A. Nilghaz, S. Bagherbaigi, C.L. Lam, S.M. Mousavi, E.P. Córcoles, D.H.B. Wicaksono, Multiple semi-quantitative colorimetric assays in compact embeddable microfluidic cloth-based analytical device (μCAD) for effective point-of-care diagnostic, Microfluid. Nanofluidics. 19 (2015) 317–333. doi:10.1007/s10404-015-1545-9.

[20] P. Wu, C. Zhang, Low-cost, high-throughput fabrication of cloth-based microfluidic devices using a photolithographical patterning technique, Lab Chip. 15 (2015) 1598–1608. doi:10.1039/C4LC01135J.

[21] W. Guan, M. Liu, C. Zhang, Electrochemiluminescence detection in microfluidic cloth-based analytical devices, Biosens. Bioelectron. 75 (2016) 247–253. doi:10.1016/j.bios.2015.08.023.

[22] G. Baysal, S. Önder, I. Göcek, L. Trabzon, H. Kızıl, F.N. Kök, et al., Microfluidic device on a nonwoven fabric: A potential biosensor for lactate detection, Text. Res. J. 84 (2014) 1729–1741. doi:10.1177/0040517514528565.

[23] R.S.P. Malon, K.Y. Chua, D.H.B. Wicaksono, E.P. Córcoles, Cotton fabric-based electrochemical device for lactate measurement in saliva., Analyst. 139 (2014) 3009–3016. doi:10.1039/c4an00201f.

[24] J.M. Cabot, N.P. Macdonald, S.C. Phung, M.C. Breadmore, B. Paull, Fibre-based electrofluidics on low cost versatile 3D printed platforms for solute delivery, separations and diagnostics; from small molecules to intact cells, Analyst. 141 (2016) 6422–6431. doi:10.1039/C6AN01515H.

[25] S. Ramesan, A.R. Rezk, K.W. Cheng, P.P.Y. Chan, L.Y. Yeo, Acoustically-driven thread-based tuneable gradient generators, Lab Chip. 16 (2016) 2820–2828. doi:10.1039/C5LC00937E.

[26] G. Zhou, X. Mao, D. Juncker, Immunochromatographic assay on thread, Anal. Chem. 84 (2012) 7736–7743. doi:10.1021/ac301082d.

[27] X. Mao, T.-E. Du, L. Meng, T. Song, Novel gold nanoparticle trimer reporter probe combined with dry-reagent cotton thread immunoassay device for rapid human ferritin test, Anal. Chim. Acta. 889 (2015) 172–178. doi:10.1016/j.aca.2015.06.031.

[28] D.R. Ballerini, X. Li, W. Shen, An inexpensive thread-based system for simple and rapid blood grouping, Anal. Bioanal. Chem. 399 (2011) 1869–1875. doi:10.1007/s00216-010-4588-5.

[29] S.S. Banerjee, A. Roychowdhury, N. Taneja, R. Janrao, J. Khandare, D. Paul, Chemical synthesis and sensing in inexpensive thread-based microdevices, Sensors Actuators, B Chem. 186 (2013) 439–445. doi:10.1016/j.snb.2013.06.036.

[30] T.-E. Du, Y. Wang, Y. Zhang, T. Zhang, X. Mao, A novel adenosine-based molecular beacon probe for room temperature nucleic acid rapid detection in cotton thread device, Anal. Chim. Acta. 861 (2015) 69–73. doi:10.1016/j.aca.2014.12.044.

[31] X. Mao, T.-E. Du, Y. Wang, L. Meng, Disposable dry-reagent cotton thread-based point-of-care diagnosis devices for protein and nucleic acid test, Biosens. Bioelectron. 65 (2015) 390–396. doi:10.1016/j.bios.2014.10.053.

[32] A. Nilghaz, D.R. Ballerini, X.Y. Fang, W. Shen, Semiquantitative analysis on microfluidic thread-based analytical devices by ruler, Sensors Actuators B Chem. 191 (2014) 586–594. doi:10.1016/j.snb.2013.10.023.

[33] M.F. Ulum, L. Maylina, D. Noviana, D.H.B. Wicaksono, EDTA-treated cotton-thread microfluidic device for one-step whole blood plasma separation and assay, Lab Chip. 16 (2016) 1492–1504. doi:10.1039/C6LC00175K.

[34] A. Gonzalez, M. Gaines, F.A. Gomez, Thread-based microfluidic chips as a platform to assess acetylcholinesterase activity, Electrophoresis. (2017). doi:10.1002/elps.201600476.

[35] F. Lu, Q. Mao, R. Wu, S. Zhang, J. Du, J. Lv, A siphonage flow and thread-based low-cost platform enables quantitative and sensitive assays, Lab Chip. 15 (2015) 495–503. doi:10.1039/C4LC01248H.

[36] A. Gonzalez, L. Estala, M. Gaines, F.A. Gomez, Mixed thread/paper-based microfluidic chips as a platform for glucose assays., Electrophoresis. 37 (2016) 1685–1590. doi:10.1002/elps.201600029.

[37] Y.A. Yang, C.H. Lin, Multiple enzyme-doped thread-based microfluidic system for blood urea nitrogen and glucose detection in human whole blood, Biomicrofluidics. 9 (2015) 22402. doi:10.1063/1.4915616.

[38] D. Agustini, M.F. Bergamini, L.H. Marcolino-Junior, Low cost microfluidic device based on cotton threads for electroanalytical application, Lab Chip. 16 (2016) 345–352. doi:10.1039/C5LC01348H.

[39] Y.C. Wei, L.M. Fu, C.H. Lin, Electrophoresis separation and electrochemical detection on a novel thread-based microfluidic device, Microfluid. Nanofluidics. 14 (2013) 583–590. doi:10.1007/s10404-012-1076-6.

[40] Y. Yan, B. Kou, L. Yan, Thread-based microfluidic three channel device in combination with thermal lens detection for the determination of copper and zinc, Anal. Methods. 7 (2015) 8757–8762. doi:10.1039/C5AY01458A.

[41] T. Wu, T. Xu, L.-P. Xu, Y. Huang, W. Shi, Y. Wen, et al., Superhydrophilic cotton thread with temperature-dependent pattern for sensitive nucleic acid detection, Biosens. Bioelectron. 86 (2016) 951–957. doi:10.1016/j.bios.2016.07.041.

[42] A.C. Glavan, A. Ainla, M.M. Hamedi, M.T. Fernández-Abedul, G.M. Whitesides, Electroanalytical Devices with Pins and Thread, Lab Chip. 16 (2015) 112–119. doi:10.1039/C5LC00867K.

[43] F. Cui, M. Rhee, A. Singh, A. Tripathi, Microfluidic Sample Preparation for Medical

Diagnostics., Annu. Rev. Biomed. Eng. 17 (2015) 267–86. doi:10.1146/annurev-bioeng-071114-040538.

[44] N.E. Manicke, B.J. Bills, C. Zhang, Analysis of biofluids by paper spray MS: advances and challenges, Bioanalysis. 8 (2016) 589–606. doi:10.4155/bio-2015-0018.

[45] S. Ulrich, Solid-phase microextraction in biomedical analysis, J. Chromatogr. A. 902 (2000) 167–194. doi:http://dx.doi.org/10.1016/S0021-9673(00)00934-1.

[46] W.A. Hassanain, E.L. Izake, M.S. Schmidt, G.A. Ayoko, Gold nanomaterials for the selective capturing and SERS diagnosis of toxins in aqueous and biological fluids, Biosens. Bioelectron. 91 (2017) 664–672. doi:http://dx.doi.org/10.1016/j.bios.2017.01.032.

[47] A.K. Yetisen, M.S. Akram, C.R. Lowe, Paper-based microfluidic point-of-care diagnostic devices., Lab Chip. 13 (2013) 2210–51. doi:10.1039/c3lc50169h.

[48] World Health Organization, List of Essential Medicines, (n.d.) Retrieved 8 December 2016.

[49] W. Wang, F. Zhou, L. Zhao, J.-R. Zhang, J.-J. Zhu, Measurement of electroosmotic flow in capillary and microchip electrophoresis, J. Chromatogr. A. 1170 (2007) 1–8. doi:10.1016/j.chroma.2007.08.083.

[50] Y. Shakalisava, M. Poitevin, J.-L. Viovy, S. Descroix, Versatile method for electroosmotic flow measurements in microchip electrophoresis., J. Chromatogr. A. 1216 (2009) 1030–1033. doi:10.1016/j.chroma.2008.12.029.

[51] F. Kohlrausch, Ueber Concentrations-Verschiebungen durch Electrolyse im Inneren von Lösungen und Lösungsgemischen, Ann. Phys. 298 (1897) 209–239. doi:10.1002/andp.18972981002.

[52] L. Hu, X. Yang, C. Wang, H. Yuan, D. Xiao, Determination of riboflavin in urine and beverages by capillary electrophoresis with in-column optical fiber laser-induced fluorescence detection, J. Chromatogr. B. 856 (2007) 245–251. doi:10.1016/j.jchromb.2007.06.011.

[53] K. Kanamaru, Correlation between water sorption and lowering of ζ-potential of fibers in water, Kolloid-Zeitschrift. 168 (1960) 115–121.

[54] L.A. Wishner, Light-induced Oxidations in Milk, J. Dairy Sci. 47 (1964) 216–221. doi:10.3168/jds.S0022-0302(64)88624-0.

593 **FIGURE CAPTION**

594

595 **Figure 1.** CAD drawing, illustration of the sizes (in millimeters), and picture of the a) reservoir
596 and b) platform features. Thread goes from the front part along the lined space, underneath
597 the rolls and tied in the ring at the back side. The perpendicular cylinder is used as a support
598 for the electrode. c) Photograph of the 3D printed fluidic platform for thread-based
599 microfluidics. The designed based on modular system allows rapid assembly of desired
600 structure and multiplexed analysis. It fits perfectly onto the microscope stage, and has a
601 rectangular hole to allow the focus of the objective lens to the thread and target detection.
602 Buffer chamber is detachable from the platform, facilitating thread cleaning and buffer
603 replenishment processes.

604 **Figure 2.** SEM of the a) threads, b) filaments, and c) cross-section. i) Nylon bundle, ii) silk, iii)
605 cotton, iv) wool, v) acrylic, vi) 50% acrylic and 50% nylon, vii) polyester, viii) waxed tape.

606 **Figure 3.** a) The Ohm's law dependence of the solution conductivity. Relationship between
607 current and electric field for polyester (■), cotton (■), waxed tape (■), silk (■), wool (●),
608 acrylic/nylon (●), nylon bundle (●), acrylic (●) threads. n=3. b) Relationship between current
609 and thread cross section area for an applied electric field of (●) 100, (■) 200, (♦) 300, and (▲)
610 400 V/cm. PES: Polyester (light blue); CO: Cotton (dark blue); WT: Waxed tape (purple); SE:
611 Silk (grey); WO: Wool (blue); AC/NYL: Acrylic/Nylon (orange); AC: Acrylic (green); NYL:
612 Nylon bundle (red). c) Electroosmotic (■) and apparent mobilities of rhodamine 6G (♦),

613 rhodamine B (●), and fluorescein (▲) for the 8 different types of threads. Error bars are based

614 on the standard deviation of 3 replicates.

Figure 4. Optimized conditions for the sample loading strategies studied: 1) a two-step standard loading and separation; 2) a two-step loading and separation with cross-pinching and pull-back, respectively; 3) a two-step standard loading and pull-back separation using lower diameter in the loading channel; 4) dropping off the sample directly onto a single separation thread.

Figure 5. a) Electromigration of riboflavin on a single nylon bundle. 0.5 μL of 5 μg/mL of standard solution of riboflavin was drop off from automatic digital syringe. b) Electropherogram on thread of 5 consecutive assays of 5 μg/mL of riboflavin solution without washing steps between sample loadings. Loading was carried out every 45 seconds. c) Electropherogram on thread of a riboflavin standard of 5 μg/mL after 1 hour exposure of sunlight. Analytes are numbered in decreasing order of mobility towards the cathode: (1) riboflavin; (2) lumiflavin; (3) lumichrome; and (4) carboxymethylflavin.

Figure 6. a) Electropherograms from thread electrophoresis and b) CE instrument of untreated urine (black) and untreated urine spiked with 8 μg/mL of riboflavin (grey). Samples were centrifuged and filtered before the analysis only for the CE instrument determination.

Figure 7. Determination of riboflavin in thread electrophoresis (black) and CE instrument (grey). Blank: untreated urine. Spike: untreated urine spiked with 8 μg/mL. Centrifugation and filtration steps were carried out only when measuring with the CE instrument. Error bars are based on the standard deviation of 5 replicates.

Table 1. Electroosmotic flow and apparent mobility of fluorescein, rhodamine B and rhodamine 6G in threads.

	Electroosmotic flow (10^{-8} m^2 V^{-1} s^{-1})	Apparent mobility (10^{-8} m^2 V^{-1} s^{-1})		
		Fluorescein	Rhodamine B	Rhodamine 6G
WT	6.34 ± 0.37	2.81 ± 0.19	4.84 ± 0.33	5.79 ± 0.33
NYL	6.09 ± 0.52	2.57 ± 0.40	3.29 ± 0.24	4.47 ± 0.22
AC	5.26 ± 0.43	2.77 ± 0.08	2.93 ± 0.24	3.42 ± 0.21
AC/NYL	4.82 ± 0.31	2.57 ± 0.16	3.18 ± 0.22	3.60 ± 0.19
PES	3.91 ± 0.32	1.90 ± 0.14	1.50 ± 0.10	2.87 ± 0.24
SE	3.64 ± 0.41	1.91 ± 0.11	-	-
CO	2.51 ± 0.46	-	-	-
WO	2.10 ± 0.31	-	-	-

Table 2. Sample loading and separation in single and dual-channel thread electrophoresis. See Figure 4 for setup and voltage conditions.

Loading and separation system			Electropherogram	FWHM	Peak area
1	a) Standard cross-loading b) Standard separation	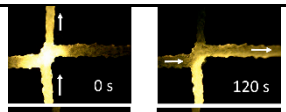	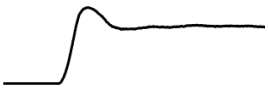	-	-
2	a) Pinching cross-loading b) Pull-back separation	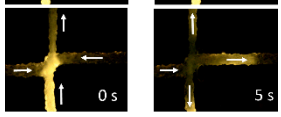		0.167	0.1720
3	a) Standard cross-loading using lower diameter b) Pull-back separation	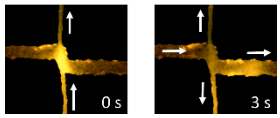	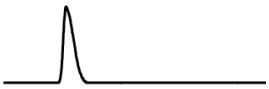	0.109	0.1128
4	a) No thread for injection b) Standard separation		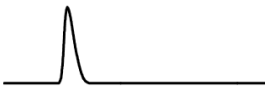	0.107	0.1142

FWHM: Full width at half maximum.